Distinct Structural Elements That Direct Solution Aggregation and Membrane Assembly in the Channel-Forming Peptide M2GlyR†

James R. Broughman,‡,§ Lalida P. Shank,‡ Wade Takeguchi,‡ Bruce D. Schultz,|| Takeo Iwamoto,‡ Kathy E. Mitchell,|| and John M. Tomich*,‡

Department of Biochemistry and Department of Anatomy and Physiology, Kansas State University, Manhattan, Kansas 66506

Received December 17, 2001; Revised Manuscript Received April 5, 2002

ABSTRACT: Restoration of chloride conductance via the introduction of an anion selective pore, formed by a channel-forming peptide, has been hypothesized as a novel treatment modality for patients with cystic fibrosis (CF). Delivery of these peptide sequences to airway cells from an aqueous environment in the absence of organic solvents is paramount. New highly soluble COOH- and NH_2-terminal truncated peptides, derived from the second transmembrane segment of the glycine receptor α-subunit (M2GlyR), were generated, with decreasing numbers of amino acid residues. NH_2-terminal lysyl-adducted truncated peptides with lengths of 22, 25, and 27 amino acid residues are equally able to stimulate short circuit current (I_{SC}). Peptides with as few as 16 amino acid residues are able to stimulate I_{SC}, although to a lesser degree. In contrast, COOH-terminal truncated peptides show greatly reduced induced I_{SC} values for all peptides fewer than 27 residues in length and show no measurable activity for peptides fewer than 21 residues in length. CD spectra for both the NH_2- and COOH-truncated peptides have random structure in aqueous solution, and those sequences that stimulated the highest maximal I_{SC} are predominantly helical in 40% trifluoroethanol. Peptides with a decreased propensity to form helical structures in TFE also failed to stimulate I_{SC}. Palindromic peptide sequences based on both the NH_2- and COOH-terminal halves of M2GlyR were synthesized to test roles of the COOH- and NH_2-terminal halves of the molecule in solution aggregation and channel forming ability. On the basis of the study presented here, there are distinct, nonoverlapping regions of the M2GlyR sequence that define solution aggregation and membrane channel assembly. Peptides that eliminate solution aggregation with complete retention of channel forming activity were generated.

Peptide-based channel replacement therapy is a potentially powerful new method for addressing human diseases such as cystic fibrosis (CF) that are caused by a loss of channel function. In the case of cystic fibrosis, currently approved conventional drug therapy addresses only symptoms such as inflammation, mucus accumulation, and chronic bacterial infections. The promise of gene therapy for treating CF appears no closer than it did 10 years ago. The newest experimental approach for treating CF, peptide-based channel replacement therapy, involves delivering a channel-forming peptide in an isotonic aqueous buffer to the apical surface of the airway epithelium (the air−cell interfacial membrane). Once bound to the target membrane, the peptide inserts across the bilayer and assembles into functional anion conductive pores.

Developing new optimized channel-forming peptides that retain channel forming activity with improved aqueous solubility and a decreased level of solution aggregation is a key objective in making "peptide-based channel replacement therapy" a reality. Throughout the search for a lead CF therapeutic, an iterative process has been employed to identify more soluble membrane active sequences that form well-behaved channels in epithelial cells.

Starting with the M2 transmembrane segment of the α-subunit of the brain glycine receptor (M2GlyR),[1] we have designed numerous novel peptide sequences that insert into lipid bilayers, whole cells, and polarized epithelial cells and assemble spontaneously into chloride-conducting pores. The solubilizing effects induced by the addition of extra lysyl residues on the COOH terminus (CK_4-M2GlyR) and the NH_2 terminus (NK_4-M2GlyR) have been described previously (*1*−*5*). Both peptides share a common, amphipathic, 23-amino

† This work is supported by the National Institute of General Medical Sciences (NIGMS) through Grant GM43617 (J.M.T.).

* To whom correspondence should be addressed: Department of Biochemistry, 103 Willard Hall, Kansas State University, Manhattan, KS 66506. Telephone: (785) 532-5956. Fax: (785) 532-6297. E-mail: jtomich@ksu.edu.

‡ Department of Biochemistry.

§ Currently in the Department of Anatomy and Physiology.

|| Department of Anatomy and Physiology.

[1] Abbreviations: M2GlyR, second transmembrane segment of the glycine receptor; AChR, acetylcholine receptor; PAGE, polyacrylamide gel electrophoresis; I_{SC}, short circuit current; DMEM, Dulbecco's modified Eagle's medium; MDCK, Madin-Darby canine kidney cells; FMOC, fluoren-9-ylmethoxycarbonyl; HMP, *p*-hydroxymethylphenoxymethyl; HPLC, high-performance liquid chromatography; MALDI-TOF MS, matrix-assisted laser desorption time-of-flight mass spectroscopy; FBS, fetal bovine serum; BS^3, bis(sulfosuccinimidyl)suberate; DMSO, dimethyl sulfoxide; HEPES, 4-(2-hydroxyethyl)piperazine-1-ethanesulfonic acid; SDS, sodium dodecyl sulfate; TFE, trifluoroethanol; NOESY, nuclear Overhauser effect spectroscopy; TOCSY, total correlation spectroscopy; 1-EBIO, 1-ethyl-2-benzimidazolinone.

10.1021/bi016053q CCC: $22.00
Published on Web 05/17/2002

acid residue core, based on residues 284−306 of M2GlyR (PARVGLGITTVLTMTTQSSGSRA), the only difference being the placement of four lysine residues on either the NH_2 or COOH terminus. This small difference is enough to alter the peptide's solubility, ability to stimulate increases in I_{SC}, and aggregation in aqueous solution. We recently showed that the carboxyl-terminally modified peptide formed a capping structure that was absent in the amino-terminally modified peptide (J. R. Broughman et al., submitted for publication). This structure was supported by chemical cross-linking, multidimensional NMR, and computer-assisted modeling. The lysyl residues on the C-terminus folded back in a capping structure in which all of the ϵ-amino groups of the added lysines formed either ionic or hydrogen bonding interactions.

Circular dichroism analysis of both the NK_4-p27 and CK_4-p27 peptides showed very similar (but not superimposable) structures (*1*). In aqueous solution, the CD spectra were consistent with an unstructured or random coil conformation. Addition of increasing concentrations of trifluoroethanol (TFE) induced both peptides to form predominantly helical structures, reaching maxima at 40% TFE. Viscosity measurements were taken in water, Ringer solution, and TFE. In water, no increase in the level of aggregation of the peptides was noted over a 6 h period. In Ringer solution, the peptides aggregated in a time-dependent manner, but with differences in rates and reaction orders. The presence of the lysyl cap on the COOH terminus greatly reduced the level of solution aggregation. NK_4-p27, however, with its lysine residues in an extended conformation without any interaction with the helical backbone of the transmembrane sequence, aggregates readily to form cross-linked complexes in excess of 50 kDa. These data suggest that there are separate and discrete sites within the molecule that contribute to aggregation and that these sites are dependent upon the secondary structure of the peptide.

Channel activity has been ascribed to homopentameric bundles of parallel M2GlyR helices (*6*, *10*). We have synthesized a series of COOH and NH_2 lysyl-modified peptides with amino acid residues deleted from the end opposite the lysine tail to better define the sites within the peptide responsible for aqueous aggregation and membrane assembly. A series of peptides based on the parent structure of the previously studied M2GlyR were prepared to determine the location of these sites. Once the sequence responsible for aggregation was localized, new palindromic sequences based on the different halves of the transmembrane M2GlyR were synthesized to confirm this assignment. The structure−activity relationships between the CK_4-M2GlyR and NK_4-M2GlyR truncated peptides and palindromes were analyzed in the context of various physical parameters. In this study, new data generated using peptides with sequence deletions further demonstrate the existence of distinct aggregation and assembly domains.

In the development of an alternative chloride conductance pathway for treating patients with CF, maximizing delivery of a membrane active species to the target cell membrane is of paramount importance. To deliver compounds to cellular targets such as the apical surface of the lung, aggregation of peptides into irreversible, nonproductive aggregates must be minimized wherever possible. Correlation of structure with aqueous aggregation and channel forming ability will aid in the design of peptide molecules with maximal activity at the shortest chain length and lowest concentration. Identifying such an optimized peptide will minimize the cost of production and maximize the therapeutic benefit of these peptides to people with anion hyposecretory disorders.

Peptides that could exist solely as monomers in solution with retention of membrane binding activity would represent a simplified system for the study of membrane-interacting peptides. One issue of primary concern to researchers studying the action of small, amphipathic peptides on their target membranes is the effect of aggregation on the ability of these molecules to bind to or insert in biological membranes. Many research laboratories currently studying peptide−membrane interactions of hydrophobic peptide sequences avoid the problem of aqueous aggregation by using low-dielectric solvents or incorporating the peptide directly with phospholipids to form proteoliposomes (*7*−*10*). Monomeric, dimeric, and higher oligomeric states are presumed to be in equilibrium, but it is not clear which forms are capable of interacting with the membrane. This limitation prevents us and others from addressing the fundamental issue of how water-soluble peptides bind to and insert across lipid bilayers.

MATERIALS AND METHODS

Peptide Synthesis. All peptides were synthesized by solid-phase synthesis using 9-fluorenylmethoxycarbonyl (FMOC) chemistry. All peptides were purified and characterized by reversed-phase HPLC and matrix-assisted laser desorption time-of-flight mass spectroscopy (MALDI-TOF MS).

Cell Culture. MDCK cells were a generous gift of L. Sullivan (Kansas University Medical Center, Kansas City, KS) and were cultured as described previously (*3*).

Electrical Measurements. Transepithelial ion transport was evaluated in a modified Ussing chamber (model DCV9, Navicyte, San Diego, CA). For electrical measurements, cells were bathed in Ringer solution (*3*) maintained at 37 °C and continuously bubbled with a 5% CO_2/95% O_2 mixture to provide aeration and mix the fluid in the chambers. The transepithelial membrane potential (V_{te}) was clamped to zero, and the transepithelial short circuit current (I_{SC}) was measured continuously with a voltage clamp apparatus (model 558C, Department of Bioengineering, The University of Iowa, Iowa City, IA). Continuous data acquisition was performed with a Macintosh computer (Apple Computer, Cuppertino, CA) using Aqknowledge software (version 3.2.6, BIOPAC Systems, Santa Barbara, CA) with an MP100A-CE interface. I_{SC} values are presented at steady-state flux levels, after the peptide has inserted into the membrane and assembled into a channel structure.

Chemical Cross-Linking Reaction for M2GlyR-Related Sequences. Bis(sulfosuccinimidyl)suberate (BS^3) was purchased from Pierce (Rockford, IL). Dimethyl sulfoxide (DMSO) was purchased from Fisher Scientific (Pittsburgh, PA). Precast 1.0 mm, 10-well, 10−20% tricine gels, the tricine SDS buffer kit, MultiMark multicolored standard, and the SilverXpress silver staining kit were obtained from Invitrogen (Carlsbad, CA). Peptides were dissolved in 1 mL of distilled water to make 1 mM stock solutions. The cross-linking reagent, BS^3, was dissolved in 0.5 μL of DMSO to make a 200 mM stock solution. In each reaction mixture,

15 μL of a 1 mM stock solution of peptide was added to 82 μL of 10 mM HEPES buffer (pH 6.5) and the mixture incubated at room temperature for 15 min. Then 3 μL of 200 mM BS^3 was then added to the previously prepared peptide solution, making a total volume of 100 μL. Each cross-linking reaction mixture contained 150 μM peptide and 6 mM BS^3, thus yielding a 40-fold molar excess of cross-linker over peptide. The peptide−cross-linker reaction was terminated by the addition of 10 μL of 1 N HCl after 30 min, and then the mixture was dried in vacuo; then 60 μL of distilled water/tricine SDS sample buffer (50:50, v/v) was added to each sample. All samples were heated at 100 °C for 5 min, and then 5 μL of each SDS-boiled sample was loaded onto the precast 10−20% tricine gel. The reference well contained 1 μL of MultiMark multicolored standard. The electrophoresis was carried out at a constant voltage of 110 V for 90 min. The gel was then visualized using silver staining.

Chemicals. 1-EBIO (Acros) was prepared as a 1 M stock solution in dimethyl sulfoxide. All other biochemicals were purchased from Sigma Chemical (St. Louis, MO) and were of reagent grade unless otherwise noted.

Data Analysis. All results are presented as means ± standard error of the mean (SEM). The difference between control and treatment data was analyzed using ANOVA and a Student's *t* test. The probability of making a type I error of <0.05 was considered statistically significant. The value of *N* is the number of independent experiments. Chi squared (X^2) is a measure of the goodness of fit of the data with the equations.

Circular Dichroism Studies. Circular dichroism was used to monitor the secondary structure of the NK_4-M2GlyR- and CK_4-M2GlyR-derived sequences in deionized and distilled water at 25 °C alone or containing 40% trifluoroethanol (TFE). Spectra were recorded on a Jasco J-720 spectropolarimeter with a Neslab RTE-111M circulator using a 1.0 mm quartz cuvette for the lower peptide concentrations and a cylindrical, water-jacketed, quartz cuvette with a 0.1 mm path length for the higher peptide concentrations. The spectra are an average of five scans recorded at a rate of 20 nm/min with a 0.2 nm step interval. Two peptide concentration ranges were employed, 30−50 and 500−600 μM. The higher concentrations cover the upper range of concentrations employed in the electrophysiological studies in MDCK monolayers. Protein concentrations were determined using the Pierce BCA micro protein assay using a calibrated M2GlyR solution as the standard. The concentration of the stock solution of NK_4-M2GlyR was determined using mole percent ratios of the hydrolyzed PTC amino acids by amino acid analysis. The data were analyzed using software provided by the manufacturer.

Molecular Simulation. Peptides were built using the Biopolymer module of Sybyl 6.7 (Tripos, St. Louis, MO). Electrostatics were assigned using the parameters developed by Kollman and co-workers (*11*). The dielectric constant was set to 4.0 for energy minimizations and dynamics simulations. The initial geometry of the peptides was assigned as α-helical. This is based on results from circular dichroism measurements of the peptides in 40% aqueous trifluoroethanol, which indicated predominantly α-helical secondary structures for the peptides.

RESULTS AND DISCUSSION

Electrophysiological Effects of the Peptides. CK_4-M2GlyR- and NK_4-M2GlyR-derived peptides (Table 1) were applied to the apical surface of MDCK cells in Ussing chambers and the respective short circuit current (I_{SC}) values determined. As the experiment is designed, increases in I_{SC} are directly related to increases in the level of anion secretion across the cell monolayer. Note that in the case of the NK_4-M2GlyR series (peptides 1−9) amino acids are sequentially removed from the C-terminus, while in the case of the CK_4-M2GlyR series (peptides 10−18), the amino acids are deleted from the N-terminus. This approach was taken to determine the minimum functional length for both the CK_4- and NK_4-M2GlyR peptides. Table 2 summarizes the electrophysiological data for the CK_4- and NK_4-M2GlyR-derived truncated sequences in columns 2 and 3. Data from 3−10

Table 1: Amino Acid Sequence, Designation, Molecular Mass, and Aqueous Solubility of the NK_4-M2GlyR- and CK_4-M2GlyR-Derived Peptides

NK_4-M2GlyR

	sequence	name	M_r (Da)	sol. (mM)
1	KKKKPARVGLGITTVLTMTTQSSGSRA	NK_4-p27	817.4	16.1
2	KKKKPARVGLGITTVLTMTTQSSGS	NK_4-p25	2590.1	15.6
3	KKKKPARVGLGITTVLTMTTQS	NK_4-p22	2358.9	11.4
4	KKKKPARVGLGITTVLTMTTQ	NK_4-p21	2271.8	8.5
5	KKKKPARVGLGITTVLTMTT	NK_4-p20	2143.7	1.6
6	KKKKPARVGLGITTVLTMT	NK_4-p19	2042.6	14.3
7	KKKKPARVGLGITTVLTM	NK_4-p18	1941.5	4.4
8	KKKKPARVGLGITTVLT	NK_4-p17	1810.3	21.2
9	KKKKPARVGLGITTVL	NK_4-p16	1709.2	11.8

CK_4-M2GlyR

	sequence	name	M_r (Da)	sol. (mM)
10	PARVGLGITTVLTMTTQSSGSRAKKKK	CK_4-p27	2817.4	13.1
11	RVGLGITTVLTMTTQSSGSRAKKKK	CK_4-p25	2649.2	22.7
12	GLGITTVLTMTTQSSGSRAKKKK	CK_4-p22	2336.8	24.6
13	LGITTVLTMTTQSSGSRAKKKK	CK_4-p21	2223.6	nd[a]
14	GITTVLTMTTQSSGSRAKKKK	CK_4-p20	2166.6	nd[a]
15	ITTVLTMTTQSSGSRAKKKK	CK_4-p19	2053.4	98.3
16	TTVLTMTTQSSGSRAKKKK	CK_4-p18	1952.3	nd[a]
17	TVLTMTTQSSGSRAKKKK	CK_4-p17	1851.2	nd[a]
18	LTMTTQSSGSRAKKKK	CK_4-p16	1752.1	98.1

[a] Not determined.

Table 2: Physical Parameters of the M2GlyR-Derived Peptides

sequence	name	I_{max} (μA cm^{-2})	$K_{1/2}$ (μM)	secondary structure
1	NK_4-p27	24.3 ± 2.5	243 ± 29.7	α-helix
2	NK_4-p25	17.6 ± 0.5	113 ± 11.9	α-helix
3	NK_4-p22	22.1 ± 0.5	169 ± 5.0	α-helix
4	NK_4-p21	17.0 ± 5.5	400 ± 55.5	α-helix
5	NK_4-p20	11.2 ± 0.3	500	α-helix
6	NK_4-p19	17.4 ± 3.1	500	nonhelical
7	NK_4-p18	13.5 ± 63.1	500	nonhelical
8	NK_4-p17	4.4 ± 0.8	393 ± 70.5	nonhelical
9	NK_4-p16	2.3 ± 10.9	500	nonhelical
10	CK_4-p27	13.1 ± 0	348 ± 142	α-helix
11	CK_4-p25	6.1 ± 0.3	323 ±7.8	α-helix
12	CK_4-p22	3.8 ± 218	500	α-helix
13	CK_4-p21	0	na[a]	nonhelical
14	CK_4-p20	0	na[a]	nonhelical
15	CK_4-p19	0	na[a]	nonhelical
16	CK_4-p18	0	na[a]	nonhelical
17	CK_4-p17	0	na[a]	nonhelical
18	CK_4-p16	0	na[a]	nonhelical

[a] Not available.

experiments were fitted by a modified Hill equation as described in the experimental methods. I_{max} values represent the maximal current, and $k_{1/2}$ represents the peptide concentration required for half-maximal activity. Decreasing the sequence length for NK_4-M2GlyR from 27 residues to 25 and 22 residues was the only truncation that resulted in decreasing $k_{1/2}$. NK_4-p25 and NK_4-p22 apparently improve channel forming activity by decreasing *K*. As previously reported (*3*, *12*), the full-length CK_4-p27 is only one-half as effective at inducing I_{SC} as the corresponding NK_4-p27. In the CK_4-M2GlyR series of peptides, the polylysine tail is at the negative end of the helix macrodipole, reducing the overall dipole of the molecule. The carbonyl oxygen atoms point toward the COOH terminus of the molecule, providing a potential site for interaction with the ϵ-amino group of the lysine molecules. In a helical structure, the side chains of the amino acids wrap back toward the NH_2 terminus. In addition, this could result in a peptide that is effectively shorter than the corresponding NH_2-terminal adduct (J. R. Broughman et al., submitted for publication). These structural differences could account for the decrease in activity, particularly if the residues that interact with the lysine cap are involved in assembling or stabilizing the helix bundles. The CK_4-p25 and CK_4-p22 truncated peptides do not retain the level of activity seen with the CK_4-p27 peptide, as is the case with the NK_4-M2GlyR peptides.

Data presented in Figure 1A show the dependence of current on peptide concentration, measured for the different NK_4-M2GlyR truncated peptides in MDCK cell monolayers. Maximal currents of $\sim$20 $\mu A/cm^2$ are observed for NK_4-p27, NK_4-p25, and NK_4-p22. The NK_4-p25 peptide reaches maximal stimulation at the lowest concentration (200 μM), while all other sequences fail to reach plateau levels even at 500 μM, the greatest concentration that was tested. The ability of only the NK_4-p25 peptide to reach a plateau with respect to inducible current suggests a more highly cooperative process. At this time, we have no indication as to which step (binding, association, insertion, or assembly) drives this process. Figure 1B summarizes the data for three concentrations (100, 300, and 500 μM). Although well within the solubility of the peptides (column 4 in Table 2), 500 μM was selected as the greatest concentration to be tested because concentrations above 1.0 mM cause aberrant electrophysiological responses to occur. The basolateral potassium channel activator 1-ethyl-2-benzimidazolinone (1-EBIO) was included in all experiments as this K^+ channel agonist increases the level of Cl^- secretion by severalfold. The behavior of the full-length peptides in the presence of this activator has been presented elsewhere (*3*, *4*). From the summarized data in Figure 1B, it is apparent that removing the first five C-terminal residues has no statistically significant effect on the measured maximal current at all concentrations. Shorter peptides, however, are associated with a reduced maximal activity when measured at 500 μM. Activity was observed with all truncated peptides that have more than 16 residues. Peptides fewer than 15 amino acids in length were inactive.

The concentration dependence of activity for the CK_4-M2GlyR-derived truncations is shown in Figure 2. CK_4-M2GlyR-derived truncations induced an increased I_{SC} when applied to the apical surface of MDCK, but only when the polypeptide chain was longer than 22 residues. Another difference between the activity versus concentration curves for the CK_4 and NK_4 truncated series is the fact that the activity curves of the CK_4-M2GlyR peptides show no signs of saturation over the tested peptide concentration range. This observation suggests some property of CK_4-p27 prevents it from achieving a maximal response even at the highest tested concentrations. The most likely explanation is that NH_2-terminal deletions eliminate residues required for directing assembly of the helical bundle. Other possible reasons for this effect include the fact that the CK_4-M2GlyR peptides are significantly more soluble in water than their NK_4-M2GlyR counterparts (column 4 of Table 2). Higher solubility for the CK_4 series could easily reduce membrane activity, thereby reducing the likelihood of binding to and inserting across the lipid bilayers. A third possibility is that the lysine capping structure at the COOH terminus could mask part of the assembly-directing site and thereby affect the affinity of the peptide segments for each other.

The concentration dependence of NK_4-M2GlyR is well-described by a modified Hill equation in that it exhibits an apparent cooperativity and yields a Hill coefficient of 2.1 ($R^2 = 0.9997$ and $\chi^2 = 0.028$). The NK_4-M2GlyR curve appears to be nearing a saturating concentration. It is not possible to determine from these data whether the NK_4 series of peptides assembles more readily or if there is a higher concentration of the monomeric peptide. Data suggest that higher concentrations of both NK_4- and CK_4-M2GlyR would yield greater activity with either peptide.

Circular Dichroism Studies. CD was used to analyze the secondary structure of the truncated peptides. The presence of the C-terminal capping structure in the CK_4-M2GlyR series of truncations suggests that these peptides have shorter end-to-end distances. Thus, truncations could reduce the overall length such that these deletion sequences might not be able to span the membrane. Before modeling could be attempted, it was important to identify the underlying secondary structure of these shortened peptides.

Data are presented in Figure 3A showing the CD spectra for most of the NK_4 deletion series in 40% aqueous TFE at concentrations ranging from 30 to 50 μM. The longer peptides (p27, p25, p22, and p21) have identical overlapping spectra that are predominantly α-helical, although some β-structure is present. More substantial structural differences are seen with sequences with fewer than 20 residues. The NK_4-p18 peptide shown in Figure 3A is clearly not helical, displaying a propensity for β or extended structural conformations. The reason for this structural aberration is unclear. NK_4-p18 has a hydrophobic residue (methionine) at the C-terminus, whereas all other peptides greater than p17 have hydrophilic residues at the C-terminus. Having a hydrophobic residue that is also a strong β-inducing amino acid at the C-terminus could be contributing to this observed shift in secondary structure in 40% TFE. The p18 peptide appears to follow the trend line for activity (Figure 1B), suggesting that its structure when bound to the membrane is not dissimilar to that of flanking truncated peptides. The activity data suggest that the CD data may indeed be an artifact.

The inset of the figure shows the CD spectra for NK_4-p25 and NK_4-p19 at concentrations greater than 500 μM. Higher peptide concentrations were checked for alterations in secondary structure because these concentrations better represent the concentrations required for electrophysiological

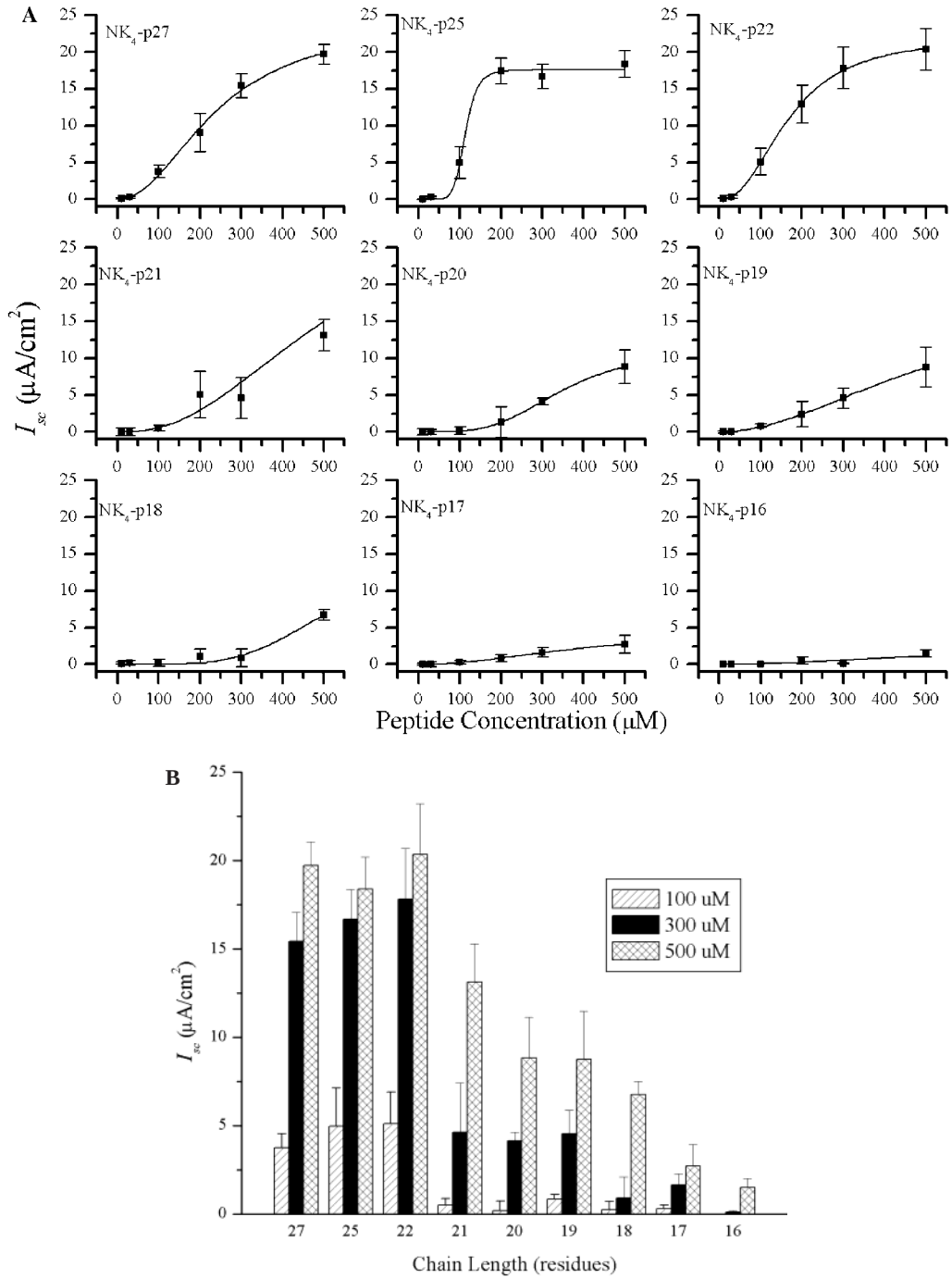

FIGURE 1: (A) Concentration dependence of I_{SC} induced by NK_4-M2GlyR peptides on MDCK epithelial monolayers. Symbols represent the mean and standard error of three to seven observations for each concentration that was tested. Solid lines represent the best fit of a first-order exponential function. Parameters of the fitted lines are given in Table 2. (B) Summary of I_{SC} values induced by NK_4-M2GlyR peptides on MDCK epithelial monolayers at total peptide concentrations of 100, 300, and 500 μM. Symbols represent the mean and standard error of three to ten observations for each concentration that was tested.

responses. Although minor increases in β-structure content are observed at the relevant physiological concentration, secondary structure does not appear to be greatly influenced by higher peptide concentrations. Previously reported data (*1*) showed that aggregation is negligible below millimolar concentrations.

Clearly, in the case of the M2GlyR sequences, maximal activity is associated with those sequences capable of existing predominantly as helical peptides in 40% TFE. It should be noted that the structures recorded in 40% TFE need not reflect the secondary structure of the peptides associated with membranes. Importantly, the ability of these peptides to adopt predominantly helical structure in TFE correlates well with the ability of the peptides to produce channels with large anion conducting potential.

The structures responsible for the reduced activities observed with the shorter peptides (<20 residues) are unknown and are beyond the scope of this report. One might speculate that these shorter sequences could be assembling into β-barrels. Such a conformation would allow the peptides to span the bilayer. $\alpha-\beta$ transitions have been observed for some of these sequences at elevated temperatures and in

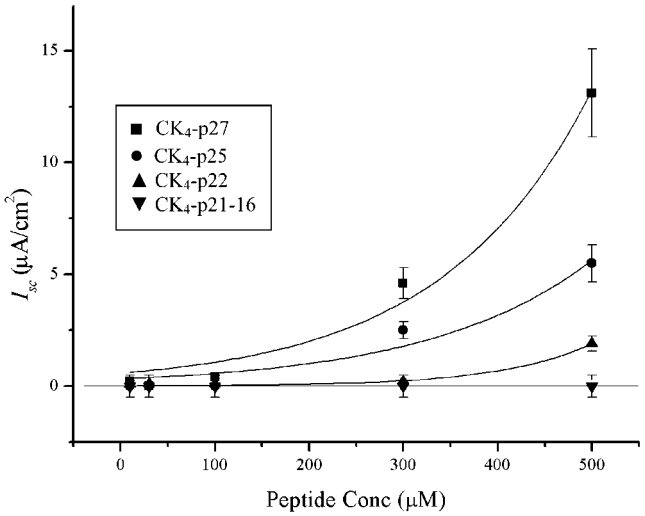

FIGURE 2: Concentration dependence of I_{SC} induced by CK_4-M2GlyR peptides on MDCK epithelial monolayers. Symbols represent the mean and standard error of three to seven observations for each concentration that was tested. Solid lines represent the best fit of a first-order exponential function. Parameters of the fitted lines are given in Table 2.

different lipid/detergent environments (unpublished observation). A minimum of eight amino acids are required to span a lipid bilayer in a β-sheet conformation, rather than the 20 residues needed for an α-helix.

The CD spectra of the CK_4 series of peptides are shown in Figure 3B. The representative spectra of active CK_4-GlyR peptides (CK_4-p27, CK_4-p25, and CK_4-p22) are identical and appear to be mostly helical. CK_4-GlyR peptides with 21 or fewer residues exhibit an increased propensity for random coil structure. The CK_4 series of peptides appears to have less α-helical structure than the corresponding NK_4 peptides based on the molar ellipticity at 222 and 208 nm. This is in agreement with the NMR studies that indicate an interaction of the lysine tail with internal residues of the peptide (J. R. Broughman et al., submitted for publication). If the CK_4 truncations form this turn, of necessity there will be fewer residues in a helical conformation. The structural changes in helical propensity do, however, correlate well with the observed activity profiles for the peptides. The inset of Figure 3B shows the CD spectra for CK_4-p22 and CK_4-p19 at concentrations greater than 500 μM. Again, secondary structure does not appear to be influenced by peptide concentration for the given representative peptides, as shown in the inset.

Modeling Studies. Starting from the CD data that indicate that all of the active species are predominantly helical, we carried out modeling studies to estimate the end-to-end distances for the sequences that were helical. Modeling simulations of all of the active NK_4 and CK_4 molecules were built as both fully extended and α-helical structures using the biopolymer module of Sybyl (version 6.7, Tripos). Each of the molecules was modeled separately, rather than minimizing the parent 27-residue peptide and then deleting terminal atoms. The molecules were then minimized using a combination protocol of 1000 iterations of steepest descent minimization to remove prohibited contacts, followed by optimizations using the conjugate gradient method until convergence was reached (0.001 kcal mol^{-1} $Å^{-1}$). Electrostatic charges were assigned to the molecule using the united-

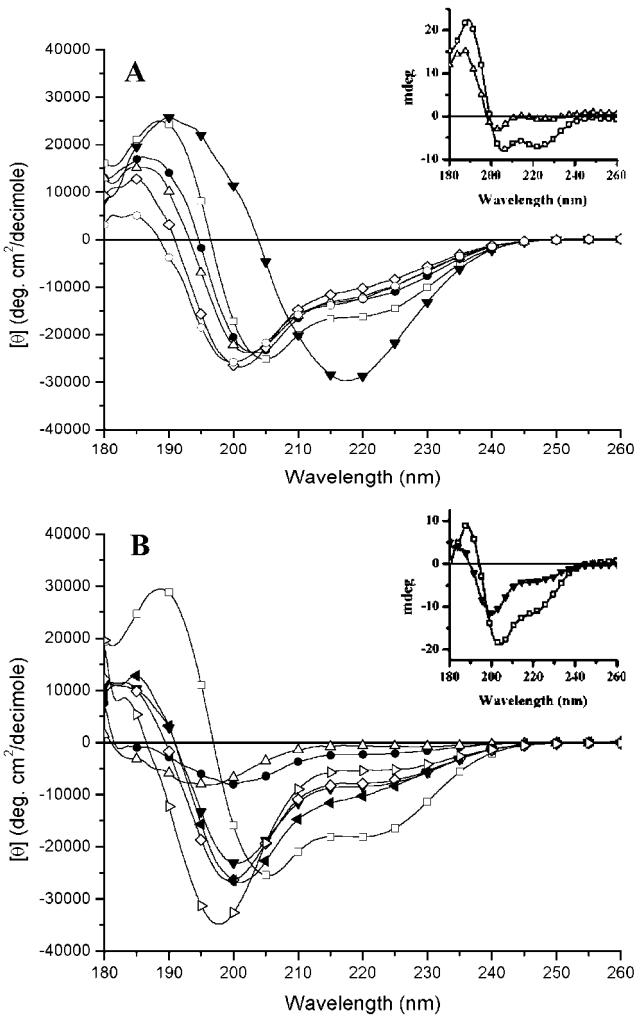

FIGURE 3: CD spectra of truncated peptides. (A) CD spectra of the NK_4 wild type (p27) and truncations (p25 and p22−p16) collected using 50 μM peptide in 40% TFE/H_2O (v/v) at room temperature (27−29 °C). CD spectra for NK_4-p27, NK_4-p25, NK_4-p22, and NK_4-p21 were averaged and plotted as one data set. CD spectra for other NK_4 peptides (p20−p16) are an average of the three data sets collected for each peptide. NK_4 peptides are as follows: average for NK_4-p27, NK_4-p25, NK_4-p22, and NK_4-p21 (□), p20 (●), p19 (△), p18 (▼), p17 (◇), and p16 (○). The inset shows CD spectra of NK_4-p25 (□) at 517 μM and NK_4-p19 (△) at 597 μM in 40% TFE/H_2O (v/v) at room temperature (27−29 °C). (B) CD spectra of the CK_4 wild type (p27) and truncations (p25 and p22−p16) collected at 50 μM peptide in 40% TFE/H_2O (v/v) at room temperature (27−29 °C). CD spectra for CK_4-p27, CK_4-p25, and CK_4-p22 were averaged and plotted as one data set. CD spectra for other CK_4 peptides (p21−p16) are an average of the three data sets collected for each peptide. CK_4 peptides are as follows: average for p27−p22 (□), p21 (●), p20 (△), p19 (▼), p18 (◇), p17 (rotated △), and p16 (rotated ▲). The inset shows CD spectra of CK_4-p25 (□) at 574 μM and CK_4-p19 (▼) at 584 μM in 40% TFE/H_2O (v/v) at room temperature (27−29 °C).

atom method of Kollman, where only explicitly required hydrogen atoms are included in the structure and all of the other hydrogens (i.e., hydrogens not involved in H-bonding) were modeled as extended portions of a carbon atom (*11*). The dielectric constant was set to 4.0. The minimized structures retained their α-helical conformation; however, unwinding of the ends was noted, especially in the NK_4 series. The distance in angstroms between the non-lysyl-adducted portion of the molecule and the α-helix carbon of the amino acid residue immediately prior to the lysine tail

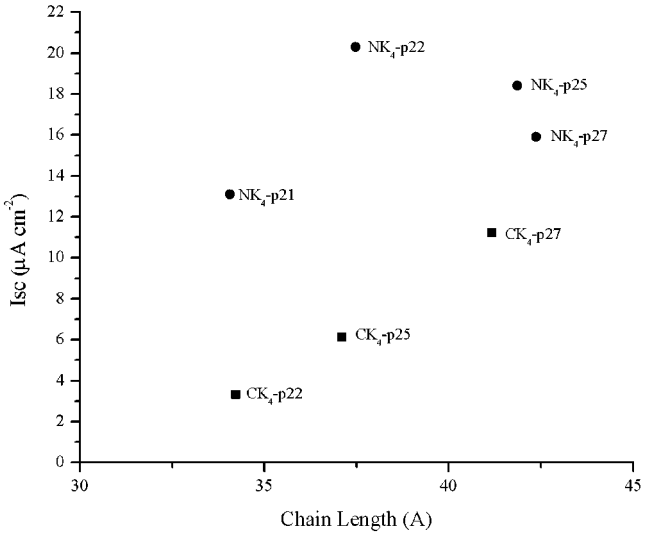

FIGURE 4: Plot of the measured short circuit current of the helical truncated peptides vs the calculated linear chain length. Models of the peptides were built using the Biopolymer module of Sybyl and energy-minimized.

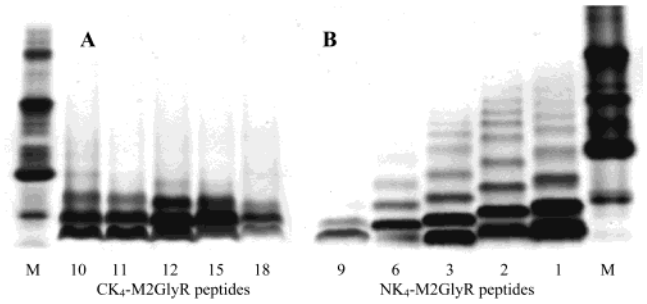

FIGURE 5: Silver-stained tricine polyacrylamide gel of cross-linking patterns for truncated and palindromic peptides. CK_4-M2GlyR (A) and NK_4-M2GlyR (B) were treated with a 40-fold excess of cross-linking reagent. M denotes the lane that contained molecular mass markers; peptides with or without treatment with BS^3 are labeled according to the sequence numbers given in Table 1.

was calculated (Pro5 in NK_4 and Ala23 in CK_4). Measured distances in the computer-generated molecules are plotted as a function of short circuit current (Figure 4). This analysis suggests that the C-capped CK_4 peptides may be considerably shorter than their paired NK_4 counterparts. CK_4-p27 is nearly 3 Å shorter than NK_4-p27. In the case of the 25-residue sequence, this difference is even more exaggerated, with CK_4-p25 close to 5 Å shorter than NK_4-p25. This difference in overall length most likely reflects the interaction of the terminal lysine residues with the helix backbone in the CK_4 truncations. All active peptides that were modeled had a length in excess of 30 Å (the distance commonly accepted for the hydrophobic thickness of a lipid bilayer). This suggests that decreased functionality was not due to peptide length. It is also important to note that the NK_4 series was able to sustain considerably higher activities as the end-to-end distance decreased. This probably reflects the ability of the lysyl butyl side chains to enter the bilayer while allowing the side chain ϵ-amino group to remain at or above the phosphoryl headgroups of the lipid molecules.

Cross-Linking Studies. Data presented in Figure 5 represent the aggregation patterns of the NK_4- and CK_4-M2GlyR series of truncation peptides in a 10 mM HEPES buffer at pH 6.5.

Table 3: Physical Parameters of the M2GlyR-Derived Palindromic Peptides

sequence	name	M_R (Da)	sol. (mM)	I_{max} (μA cm^{-2})	$K_{1/2}$ (μM)	secondary structure
19	NK_4-ALa	2774.5	4.7	25.0	50	α-helix
20	NK_4-bLB	2860.3	9.3	5.2	78	nonhelical
21	CK_4-ALa	2774.5	10.0	25	100	α-helix

An aqueous solution of peptide was cross-linked with a lysine specific cross-linker [bis(sulfosuccinimidyl)suberate]. The molecular masses of the cross-linked CK_4-M2GlyR and NK_4-M2GlyR truncated peptides are shown in panels A and B of Figure 5, respectively. NK_4-p27 and CK_4-p27 run with apparent molecular masses of 2401 and 2230 Da, respectively, values that are slightly lower than that obtained by mass spectrometry (2817 Da). Previously, we reported a small but measurable difference between the apparent molecular masses for NK_4-p27 and CK_4-p27 that appeared reproducibly (J. R. Broughman et al., submitted for publication). All peptides were analyzed after synthesis by HPLC and mass spectrometry and were determined to have the expected molecular mass. Since both peptides have the same mass as determined by time-of-flight mass spectrometry, this difference suggests a slightly more compact structure for the CK_4 peptide. Another possible explanation is a reduction in the level of SDS binding due to the loss of hydrophobic residues, which has been proposed to cause some peptides to migrate anomalously.

The degree of aggregation for the CK_4 peptides remains relatively constant throughout the series of deletions. Although the degree of aggregation appears to be rather small, it remains unchanged by varying magnitudes of N-terminal residue deletions. The NK_4-M2GlyR peptides show a much different pattern of aggregation. The level of aggregation is reduced with each new truncation such that by the time 11 C-terminal residues have been removed, little if any aggregation is observed.

These results suggest that there may be a specific nucleation site for aggregation (at least in aqueous solution) in the C-terminus of the M2GlyR sequence. This site appears to be masked in the CK_4 truncations due most likely to the C-capping of the lysine tail and serially deleted in the NK_4 peptides (J. R. Broughman et al., submitted for publication).

Design, Synthesis, and Testing of NH_2-Terminal Modular Palindromes. Either orientation of the M2GlyR helical segment has been shown previously to form functional ion channels (*1*). This observation implies a chloride ion can pass through the N-terminal half of the sequence whether it is located at the cytoplasmic or extracellular interface. Via exclusion of C-terminal sequences, aggregation should be eliminated if indeed the C-terminus is the site that nucleates aggregation. If the aggregation domain is in the C-terminal half of the molecule, it should have a reduced ability to stimulate ion transport and, obviously, aggregate in aqueous solution. To test this hypothesis, palindromic peptides comprised of either the 11 NH_2- or COOH-terminal residues followed by a sequence inversion about the central leucine and a four-lysine cap were synthesized. The resultant sequences are as follows: AARVGLGITTV-L-VTTIGLGVRAA and ARSGSSQTTMT-L-TMTTQSSGSRA (see Table 3). These sequences were assessed for solubility, aggregation, and secondary structure, as well as the ability

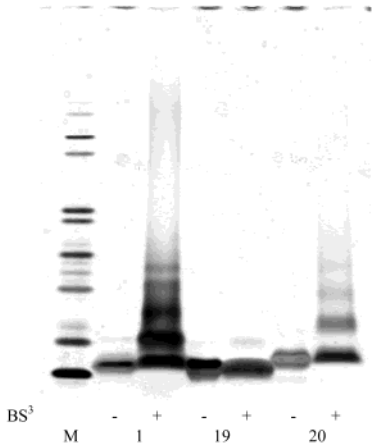

FIGURE 6: Pattern of aggregation of cross-linked palindromic peptides compared to NK_4-p27 peptides with or without treatment with BS^3 are labeled according to the sequence numbers given in Tables 1 and 3.

to stimulate I_{SC}. The proline normally found in the NH_2-terminal half of the peptide was replaced with alanine. This modification improved the synthetic yield with no apparent effect on secondary structure or channel forming properties. The properties of these sequences are shown in Table 3. On the basis of our hypothesis that the aggregation domain resides within the COOH-terminal half of the M2GlyR sequence, the NK_4-ALa palindrome should be monomeric in solution and still form anion-conducting channels in membranes, and the effective concentration should decrease if the monomeric form of the peptide is the most bioactive species.

Data presented in Figure 6 show the result of a solution cross-linking reaction for the NK_4-ALa and NK_4-bLB palindromes. Both molecules appear to be monomeric when boiled in SDS without cross-linking. After addition of the cross-linker, multiple aggregated species of NK_4-bLB are present, while NK_4-ALa appears mainly as a monomer with a faint band that corresponds to dimer but no greater aggregates. This result clearly shows that the aggregation domain lies within the COOH-terminal half of the molecule. As a control, the cross-linked peptides were analyzed by mass spectrometry prior to the addition of the SDS-containing loading buffer to confirm that they reacted with the BS^3 reagent. The mass spectra indicated that both palindromes had reacted, producing dimers and trimers with almost no monomer present (data not shown). To test for any concentration dependence on aggregation, cross-linking experiments were carried out on the NK_4-ALa palindrome using a 10-fold concentration range (30−300 μM). No increase in the level of aggregation was observed over the full range of concentrations that were tested (data not shown).

Data presented in Figure 7 show concentration-dependent effects for both palindromes. Apical application of NK_4-ALa to MDCK monolayers in the presence of 1-EBIO increases the induced I_{SC} to approximately the same magnitude as that of NK_4-p27, but at a half-maximal effective concentration of 40 μM. The NK_4 palindrome is able to form channels at the lowest concentrations ever observed for any M2GlyR-derived sequence. The CD spectra of NK_4-ALa in water and 40% TFE are presented in Figure 8. NK_4-ALa exhibits more structural content in water than any peptide designed so far

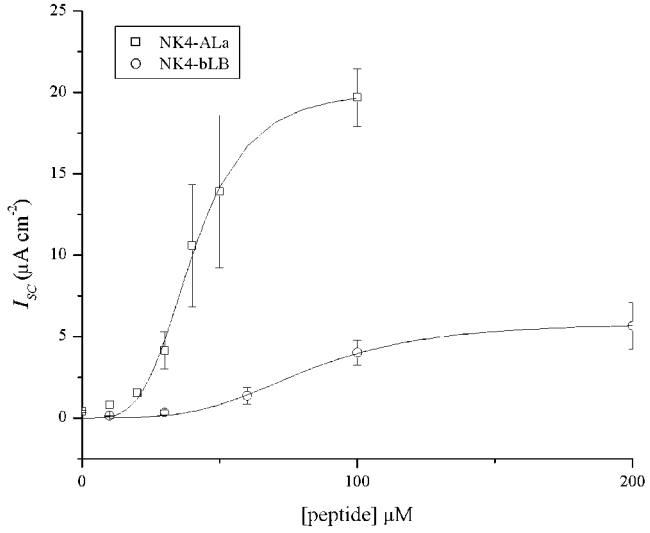

FIGURE 7: Concentration dependence of I_{SC} induced by NK_4-ALa and NK_4-bLB on MDCK epithelial monolayers. Symbols represent the mean and standard error of four to six observations for each concentration that was tested. Solid lines represent the best fit of a modified Hill equation to the data. Parameters of the fitted lines are given in Table 3.

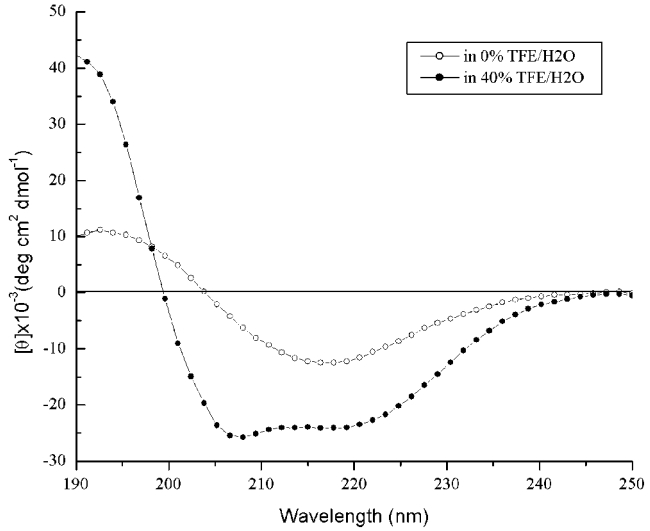

FIGURE 8: CD spectra of NK_4-ALa in H_2O (○) and 40% TFE/H_2O (v/v) (●). Spectra were collected using 50 μM peptide at room temperature (27−29 °C).

(*1*). The CD spectrum of NK_4-ALa in water has a strong minimum at 218 nm, indicating a high proportion of β-structure. The higher than expected peak at 192 nm suggests the presence of some helical segments. In 40% TFE, the population of NK_4-ALa is almost entirely in the helical state. NK_4-bLB is unstructured in water and nonhelical in 40% TFE (data not shown). NK_4-bLB was able to stimulate an increase in I_{SC} across the MDCK monolayer, but with a much lower maximal current (5.8 μA cm^{-2}). The reduced I_{SC} for NK_4-bLB is most likely due to the loss of portions of the helical bundle assembly domain, which we hypothesize resides within the NH_2-terminal half of the molecule. The CK_4-Ala palindrome is able to reach the same maximal current as the NK_4 palindrome but at a slightly higher concentration. This result suggests that placing four lysines at the C-terminus interferes with helix bundle assembly to some extent. At the higher palindrome concentrations (>80

μM), the resistance of the monolayers decreases approximately 1000-fold, an effect that has not been observed previously for other M2GlyR-derived peptides at these extremely low concentrations. The mechanism creating this phenomenon is unknown at this time. However, if the peptide is removed from the cell medium, the resistance appears to recover over time. Preliminary cytotoxicity assays also clearly indicate that the palindromes have little effect on isolated, nonpolarized IB3 or T84 cells. While the palindrome sequence suggests that channel-forming peptides can be designed that are monomeric, these sequences will probably not find use in the clinic until we fully understand how these monomeric species are reducing the resistance of the monolayers.

SUMMARY

The results presented in this report suggest that aggregation and association of the M2GlyR amphipathic molecule are separate and distinct events, the determinants of which are two different primary structural elements. Aqueous aggregation of the M2GlyR peptides involves a defined nucleation site located near the COOH terminus of the sequence. Removal of this site creates a peptide that retains the ability to bind to and insert across lipid membranes and create functional channels, at a significantly lower concentration than the parent molecule. The amino acid residues involved in the membrane assembly of the high-conductance pore appear to be located in the NH_2-terminal half of the sequence.

We have identified a novel amino acid sequence that provides predominantly monomeric peptides in solution and produces pores in membranes capable of efficiently transporting monovalent anions across epithelial monolayers. This discovery will aid in future studies of peptide−membrane interactions.

ACKNOWLEDGMENT

We are grateful to Gary Radke and Ryan Carlin for technical assistance. This work is contribution 02-235-J from the Kansas Agricultural Experiment Station (J.M.T. and B.D.S.).

REFERENCES

1. Tomich, J. M., Wallace, D., Henderson, K., Mitchell, K. E., Radke, G., Brandt, R., Ambler, C. A., Scott, A. J., Grantham, J., Sullivan, L., and Iwamoto, T. (1998) *Biophys. J. 74*, 256−267.
2. Wallace, D. P., Tomich, J. M., Iwamoto, T., Henderson, K., Grantham, J. J., and Sullivan, L. P. (1997) *Am. J. Physiol. 272*, C1672−C1679.
3. Broughman, J. R., Mitchell, K. E., Sedlacek, R. L., Iwamoto, T., Tomich, J. M., and Schultz, B. D. (2001) *Am. J. Physiol. 280*, C451−C458.
4. Wallace, D. P., Tomich, J. M., Eppler, J. W., Iwamoto, T., Grantham, J. J., and Sullivan, L. P. (2000) *Biochim. Biophys. Acta 1464*, 69−82.
5. Mitchell, K. E., Iwamoto, T., Tomich, J., and Freeman, L. C. (2000) *Biochim. Biophys. Acta 1466*, 47−60.
6. Hristova, K., Wimley, W. C., Mishra, V. K., Anantharamiah, G. M., Segrest, J. P., and White, S. H. (1999) *J. Mol. Biol. 290*, 99−117.
7. Lew, S., Ren, J., and London, E. (2000) *Biochemistry 39*, 9632−9640.
8. Marti, T. (1998) *J. Biol. Chem. 273*, 9312−9322.
9. Liu, L. P., and Deber, C. M. (1997) *Biochemistry 36*, 5476−5482.
10. Reddy, G. L., Iwamoto, T., Tomich, J. M., and Montal, M. (1993) *J. Biol. Chem. 268*, 14608−14615.
11. Singh, U., and Kollman, P. (1984) *J. Comput. Chem. 5*, 129−145.
12. Gao, L., Broughman, J. R., Iwamoto, T., Tomich, J. M., Venglarik, C. J., and Forman, H. J. (2001) *Am. J. Physiol. 281*, L24−L30.

BI016053Q